Near-IR Absorbance Changes and Electrogenic Reactions in the Microsecond-to-Second Time Domain in Photosystem I

Ilya R. Vassiliev,* Yean-Sung Jung,* Mahir D. Mamedov,[§] Alexey Yu. Semenov,[§] and John H. Golbeck*
*Department of Biochemistry, The G. W. Beadle Center, University of Nebraska, Lincoln, Nebraska 68588-0664; and [§]A. N. Belozersky Institute of Physico-Chemical Biology, M. V. Lomonosov Moscow State University, Moscow 119899, Russia

ABSTRACT The back-reaction kinetics in Photosystem I (PS I) were studied on the μs-to-s time scale in cyanobacterial preparations, which differed in the number of iron-sulfur clusters to assess the contributions of particular components to the reduction of P_{700}^{+}. In membrane fragments and in trimeric P_{700}-F_A/F_B complexes, the major contribution to the absorbance change at 820 nm (ΔA_{820}) was the back-reaction of F_A^- and/or F_B^- with lifetimes of ~10 and 80 ms (~10% and 40% relative amplitude). The decay of photoinduced electric potential ($\Delta\psi$) across a membrane with directionally incorporated P_{700}-F_A/F_B complexes had similar kinetics. $HgCl_2$-treated PS I complexes, which contain F_A but no F_B, retain both of these kinetic components, indicating that neither can be assigned uniquely to a specific acceptor. These results suggest that F_A^- reduces P_{700}^{+} directly and argue for a rapid electron equilibration between F_A and F_B, which would eliminate their kinetic distinction in a back-reaction. In PsaC-depleted P_{700}-F_X cores, as well as in P_{700}-F_A/F_B complexes with chemically reduced F_A and F_B, the major contribution to the ΔA_{820} and the $\Delta\psi$ decay is a biphasic back-reaction of F_X^- (~400 μs and 1.5 ms) with some contribution from A_1^- (~10 μs and 100 μs), the latter of which is variable depending on experimental conditions. The ΔA_{820} decay in a P_{700}-A_1 core devoid of all iron-sulfur clusters comprises two phases with lifetimes of 10 μs and 130 μs (2.7:1 ratio). The biexponential back-reaction kinetics found for each of the electron acceptors may be related to existence of different conformational states of the PS I complex. In all preparations studied, excitation at 532 nm with flash energies exceeding 10 mJ gives rise to formation of antenna ^{3}Chl, which also contributes to ΔA_{820} decay on the tens-of-μs time scale. A distinction between ΔA_{820} components related to back-reactions and to ^{3}Chl decay can be made by analysis of flash saturation dependencies and by measurements of kinetics with preoxidized P_{700}.

INTRODUCTION

The primary photochemical event in Photosystem I (PS I) is initiated by the absorption of light quanta by antenna chlorophyll molecules with subsequent energy migration to the specialized reaction center trap. Primary charge separation takes place within 14 ps between the primary donor P_{700}, a chlorophyll dimer, and the primary acceptor A_0, a chlorophyll monomer (for review see Sétif, 1992; Hastings et al., 1995). This initial step is followed by subsequent stages of charge stabilization on a series of electron carriers, including A_1 (a phylloquinone) and three [4Fe-4S] clusters, F_X, F_A, and F_B. Whereas P_{700}, A_0, A_1, and F_X are bound to the PsaA/PsaB reaction center heterodimer, the terminal clusters F_A and F_B are located on the tightly bound 8.9-kDa PsaC subunit (recently reviewed by Chitnis et al., 1995). Many of the pioneering studies in PS I were carried out by analysis of the kinetics of photoinduced optical absorbance changes of the electron-transport components, especially that of the primary donor, P_{700}. Photooxidation of P_{700} is characterized by a difference spectrum with large negative absorption changes (bleaching) around 430 and 700 nm and smaller positive absorption changes around 450 and 820 nm (Hiyama and Ke, 1972). In spite of the ca. 10-times lower extinction coefficient compared with 700 nm, the spectral region around 820 nm provides advantages for monitoring the changes in redox state of P_{700} because neither charge separation nor chlorophyll fluorescence are induced by light in this spectral region, and absorbance changes may be monitored at relatively high chlorophyll concentrations in the sample.

In the absence of soluble electron donors and acceptors, charge separation in isolated PS I preparations is followed by charge recombination with one or more of the bound electron acceptors, and can be measured by the decay of the photoinduced absorbance change of P_{700}^{+}. To summarize the existing data: in isolated PS I complexes that contain the F_A and F_B clusters as the terminal acceptors, charge recombi-

---

Received for publication 4 April 1996 and in final form 23 October 1996.

Address reprint requests to (present address) Dr. John H. Golbeck, Dept. of Biochemistry and Molecular Biology, The Pennsylvania State University, S-310 Frear Laboratory, University Park, PA 16802-4500. Tel.: 814-865-1163; Fax: 814-863-7024; E-mail: jhg5@psu.edu.

Ilya R. Vassiliev is on leave from the Department of Biophysics, Faculty of Biology, M. V. Lomonosov Moscow State University, Moscow 119899, Russia. Present address: Dept. of Biochemistry and Molecular Biology, The Pennsylvania State University, S-310 Frear Laboratory, University Park, PA 16802-4500.

Published as Journal Series #11464 of the University of Nebraska Agricultural Research Division.

The abbreviations and definitions used are: PS I, Photosystem I; Chl, chlorophyll; DCPIP, 2,6-dichlorophenol-indophenol; DM-PS I, PS I complex (containing F_X, F_A and F_B clusters) isolated using *n*-dodecyl-β-D-maltoside; ΔA_{820}, photoinduced absorbance change at 820 nm; $\Delta\psi$, photoinduced electric potential; P_{700}, the primary electron donor in PS I, a chlorophyll *a* dimer; P_{700}-A_1 core, preparation isolated from a P_{700}-F_X core by oxidative denaturation of the F_X cluster; P_{700}-F_X core, preparation isolated from a PS I complex by removal of the PsaC subunit and hence devoid of the F_A and F_B clusters; TX-PS I, PS I complex (containing F_X, F_A and F_B clusters) isolated using Triton X-100.

0006-3495/97/01/301/15 $2.00

nation takes place with a half-time of ~30 ms (lifetime of 43 ms) (Ke, 1972). The kinetics of the back-reactions of earlier electron acceptors are observed either upon chemical prereduction of the F_A and F_B clusters (Sauer et al., 1978) or in "PS I core" preparations (Golbeck, 1995). The latter are devoid of the PsaC subunit (Li et al., 1991), and depending on the isolation procedure, may also have the F_X cluster missing (Parrett et al., 1990; Warren et al., 1990). The half-time for the F_X back-reaction at room temperature was found to be 250 μs in a PS I complex with F_A/F_B reduced with dithionite (Sauer et al., 1978) or with successive flashes (Bottin et al., 1987), and 1.2 ms in a F_A/F_B-less, P_{700}-F_X core (Golbeck and Cornelius, 1986). The components ascribed to the A_1 back-reaction were reported to be 3 μs (Sauer et al., 1979), 750 ns (Bottin et al., 1987), 250 μs (Brettel, 1989), or 10 μs (Warren et al., 1993), depending on the type of preparation and the reduction protocol. A recent study made on a F_X-less, P_{700}-A_1 core shows that the A_1 back-reaction follows multiexponential kinetics, where the majority of the charge recombination occurs with half-times of ~10 μs and 150 μs (lifetimes of 15 and 217 μs) at room temperature, and with kinetics only slightly slower at liquid helium temperatures (Brettel and Golbeck, 1995). It is not clear, however, whether A_1^- can transfer electrons back to P_{700}^+ when only the terminal clusters (F_A and F_B) are prereduced or removed.

In the course of studying various mutants of PS I, we took note that the decay of the absorbance change at 820 nm (ΔA_{820}) in the μs-to-s time domain comprises a broad continuum of kinetic phases. This was particularly evident in mutants with cysteine-to-serine substitutions in the ligands to the F_X cluster (Vassiliev et al., 1995a), where multiphase kinetics were measured from both the A_1^- and the F_X^- back-reactions. In these instances, the number of phases observed was usually greater than the number of endogenous acceptors that were available to back-react with P_{700}^+. It should be noted that most previous studies of ΔA_{820} kinetics were performed using relatively narrow time scales, which were set up for a preferential monitoring of the major decay component, thus causing some minor components to be overlooked.

Another problem related to the interpretation of ΔA_{820} transients is the possible interference from the presence of chlorophyll triplet states, which decay in the μs time domain, and yet have a difference spectrum with a weak positive absorption in the near infra-red which is similar, though not identical, to the P_{700}^+ cation. Contributions from antenna species (Nuijs et al., 1986) and from $^3P_{700}$ formed in the back-reaction as intermediates between the charge-separated radical pair and the ground state of P_{700} (Sétif and Bottin, 1989; Sétif and Brettel, 1990) are possible in this time domain. It was recently shown that at least in the case of direct $P_{700}^+A_1^-$ recombination, there is no $^3P_{700}$ intermediate involved (Warren et al., 1993); it is highly likely that the back-reaction(s) of F_X, F_A, and F_B also do not proceed via $^3P_{700}$.

This work is aimed at providing a detailed comparison of room temperature ΔA_{820} kinetics in different PS I preparations using one and the same acquisition setup with a resolution in the μs-to-s time domain. The stated goal is to verify the lifetimes of existing phases and contributions of endogenous acceptors to the overall decay of P_{700}^+. We address the mechanism of the back-reaction of the terminal acceptors, F_A and F_B, in isolated PS I complexes in terms of their individual contributions to the back-reaction kinetics and the possible involvement of $^3P_{700}$ in the process. To investigate the kinetics of back-reactions from A_1 and F_X and possible interference of chlorophyll triplet states in the μs time domain, we use preparations that are devoid of different iron-sulfur clusters or have them stabilized in the reduced state. The key ΔA_{820} experiments are paralleled by measurements of the photoinduced electric potential ($\Delta\psi$) across a phospholipid bilayer membrane reconstituted with directionally oriented PS I complexes.

MATERIALS AND METHODS

Cell growth and isolation of thylakoid membranes, PS I complexes, and PS I cores

A glucose-tolerant strain of *Synechocystis* sp. PCC 6803 was grown at 30°C in BG-11 medium with 5 mM glucose under light-activated heterotrophic growth conditions in the dark, as previously described (Anderson and McIntosh, 1991). Thylakoid membranes were isolated according to Smart et al. (1991). PS I trimeric complexes from *Synechocystis* sp. PCC 6803 (DM-PS I) were isolated using *n*-dodecyl-β-D-maltoside (β-DM) as described earlier (Warren et al., 1993), with minor modifications (Vassiliev et al., 1995a). PS I trimeric complexes from *Synechococcus* sp. PCC 6301 (TX-PS I) were isolated with Triton X-100. PS I core preparations (P_{700}-F_X cores and P_{700}-A_1 cores) were isolated from DM-PS I or TX-PS I complexes as summarized in Golbeck (1995). Isolated PS I preparations were resuspended in 50 mM Tris buffer, pH 8.3, with 15% glycerol, frozen as small aliquots in liquid nitrogen, and stored at −95°C. Hg-treated TX-PS I complexes, which are devoid of the F_B cluster, were isolated as described in Jung et al. (1995), an adaptation to cyanobacteria of the original protocol (Sakurai et al., 1991).

Near-IR kinetic spectroscopy

Samples for optical experiments were suspended to a Chl *a* concentration of 30–50 μg ml^{-1} in 25 mM Tris buffer (pH 8.3) in a 10 mm × 2 mm quartz cuvette with a stopper. β-DM or Triton X-100 were added to a final concentration of 0.04% to reduce light scattering. DCPIP and sodium ascorbate (both from Sigma, St. Louis, MO) were added where indicated. For chemical reduction of the F_A and F_B clusters, the samples were suspended in 100 mM glycine buffer, pH 10.0, with 100 mM sodium dithionite (Sigma). Unless otherwise indicated, all solutions were prepared in an anaerobic chamber using oxygen-free distilled water, air being substituted in a Thumberg tube by high-purity nitrogen gas (Air Products, Allentown, PA).

Transient absorbance changes of P_{700} at 820 nm (ΔA_{820}) were measured from the μs to tens-of-seconds time domain using a laboratory-built double-beam spectrometer as described previously (Vassiliev et al., 1995a), but with some modifications. In most of the experiments, the voltages from the measuring and reference photodiodes were directed to the noninverting and inverting inputs of a DC-coupled differential amplifier (Model 113, EG&G, Princeton, NJ) which was set to a high frequency roll-off of either 100 kHz or 300 kHz. The difference signal was amplified with a Tektronix 11A52 DC-coupled plug-in and digitized with a Tektronix

DSA 601 digital signal analyzer (Tektronix, Beaverton, OR). For faster time resolution the signals from the measuring and reference photodetectors were directed into a Tektronix 11A33 differential amplifier plug-in (1 MΩ impedance, 20 MHz bandwidth). Data were acquired on two different time scales using zoom window capacities of the DSA 601. In different sets of experiments the main sample interval was set from 100 μs to 1 ms per point, and the zoom window interval was set from 1 μs to 10 μs per point. Each set of traces was stored in the DSA 601 memory, transferred to a Macintosh Quadra (68040/40 MHz) computer via a National Instruments NB-GPIB/TNT board, and saved in separate files. The ΔA_{820} values were calculated as $0.434 \times \Delta I/I$, where I is the intensity of the measurement laser beam monitored as the output photovoltage of the detector and ΔI is the light-induced change.

The flash excitation was provided by a frequency-doubled, Q-switched DCR-11 Nd-YAG laser (Spectra-Physics, Mountain View, CA) operating at 532 nm with the pulse FWHM of 10 ns. The flash energy (up to 150 mJ) was controlled by varying the Q-switch delay and/or using neutral density filters. Preillumination flashes were provided by a Model 6100E-72 Xenon flash lamp (Photochemical Research Associates, London, ON, Canada). The flash width at half-maximum was 10 μs, and flash energy was ~5 mJ. A light guide was used to direct the flash light to the side of the cuvette opposite to that illuminated by the Nd-YAG laser. Flashes trains consisted of successive firing spaced at 15-ms intervals, including the terminal YAG laser flash. The saturating intensity of the flash was confirmed using neutral density filters and monitoring the ΔA_{820} signal.

Steady-state excitation at 710 nm was provided by a TI-SPB titanium-sapphire laser (Schwartz Electro-Optics, Orlando, FL) pumped with a Spectra Physics Model 2020-05 argon ion laser emitting all-lines at 5 W output power. The far-red excitation beam was passed through a fivefold beam expander, chopped at appropriate intervals using a Uniblitz VS25 shutter (Vincent Associates, Rochester, NY) and diverted to the cuvette with a light guide to provide incident light energy of 20 mW.

Transmembrane electric potential

Incorporation of PS I complexes and cores into proteoliposomes was carried out at 4°C as described in Mamedov et al. (1995): soybean lecithin (Type II-S, Sigma) was dispersed to 10 mg ml^{-1} in the buffer solution of 20 mM Tris, pH 8.0 with 2 mM $MgCl_2$. The lipid solution was sonicated in a UZDN-2T ultrasonic disintegrator in 10-s bursts (50 mA, 22 kHz) up to an overall sonication time of 2 min under argon atmosphere. The clear phospholipid solution was mixed with PS I complexes and sonicated for 20 s. The lipid/chlorophyll ratio was 125:1.

Measurements of transmembrane $\Delta\psi$ generated by PS I-containing proteoliposomes absorbed onto the surface of asolectin-impregnated collodion film were done under argon atmosphere at room temperature as described elsewhere (Drachev et al., 1979). The proteoliposome suspension was added to one of the two compartments of a Teflon cuvette filled with buffer. A collodion film impregnated with a 10% (w/v) asolectin in *n*-decane was used as a separator between the compartments. Association of vesicles with the collodion film was achieved upon 1–1.5 h incubation in the presence of 20 mM $CaCl_2$ at room temperature. Subsequently both compartments were washed with a 10-fold volume of the same buffer to remove excess proteoliposomes and $CaCl_2$. The $\Delta\psi$ generated across the collodion film was measured with two light-protected Ag/AgCl electrodes connected to an operational amplifier (Burr-Brown 3554 BM). The electric signals were digitized with a transient recorder DL-1080 (DataLab, UK), interfaced to an IBM-compatible computer, and stored in files. The instrument time constant was 200 ns. Light flashes were provided by a frequency-doubled Quantel Nd-YAG laser (wavelength, 532 nm; FWHM, 15 ns; flash energy, 40 mJ).

Kinetic analysis

The ΔA_{820} and $\Delta\psi$ traces for each time window were averaged, where required, and non-overlapping parts of traces corresponding to different time domains were linked to yield an overall decay curve using Igor Pro 2.04 (WaveMetrics, Lake Oswego, OR). In most instances, the total number of points was reduced to 6144 by interpolating the set of points starting from the 2049th point to a log-distributed time scale vector. The ΔA_{820} and $\Delta\psi$ kinetics were fitted using the Marquardt algorithm in Igor Pro to sum of up to seven exponentials with a baseline with all amplitudes and rate constants set free during the fit or to sum of three exponentials with global lifetimes (experiment presented in Fig. 8). The results of the fit were automatically output as the overall fit curve, individual components curves, residuals, and values of lifetimes and amplitudes components and their standard errors. In most cases the fit comprised a baseline component accounting for long-term phases and/or possible drift of signal zero during long-time scale acquisition. For more explicit presentation of the results each individual component was plotted with a vertical offset relative to the next component (with a longer lifetime) or to the baseline, the offset being equal to the amplitude of the latter component. Therefore, with components plotted on the log time scale and with an auxiliary percentage axis (with 100% equal to the overall initial amplitude) the vertical offsets between the components should also represent the percentages of the individual components. The quality of the fit was estimated using standard techniques including analyses of the residuals plots and comparison of the χ^2 values and standard errors of the fit parameters between different fits (not shown).

RESULTS

P_{700}-F_A/F_B Complex

The initial set of studies involved the kinetics of ΔA_{820} in various PS I preparations that contain the entire electron transport complement from P_{700} to the terminal iron sulfur clusters, F_A and F_B. Excitation flashes were provided at a 50-s repetitive rate at appropriate donor (reduced DCPIP) concentrations (see below), conditions which allowed nearly complete relaxation of the ΔA_{820} signal. Inasmuch as the averaging was performed only after the data were downloaded to the computer, this protocol enabled monitoring of the individual kinetic traces during the course of successive excitations. The kinetics are displayed on a logarithmic rather than on a linear time scale because this method of presentation provides a much better visualization of the decay times involved, even before computer-aided analysis. To verify the validity of the multiexponential computer-aided analysis, we have made decompositions of selected kinetic traces with other nonlinear regression software (PeakFit by Jandel Scientific), which gave identical results to Igor Pro, but we found the latter more suitable in terms of customization to our application.

ΔA_{820} decay phases in P_{700}-F_A/F_B complexes

Fig. 1 *A* shows the ΔA_{820} kinetics from a DM-PS I complex averaged after 12 repetitive flashes; Fig. 1 *B* depicts the kinetics in the absence of exogenous electron donors. Because an artificial electron donor (such as DCPIP reduced by sodium ascorbate) is required for complete reduction of P_{700}^{+} in the dark intervals between the flashes (Ke, 1972), the overall amplitude of ΔA_{820} is much lower in the absence of such a donor than in its presence. As shown in Fig. 1 *A*, the majority of the absorbance change in a DM-PS I complex decays in the tens-of-ms time domain. The first kinetic trace acquired in the 12-flash sequence was found to be very

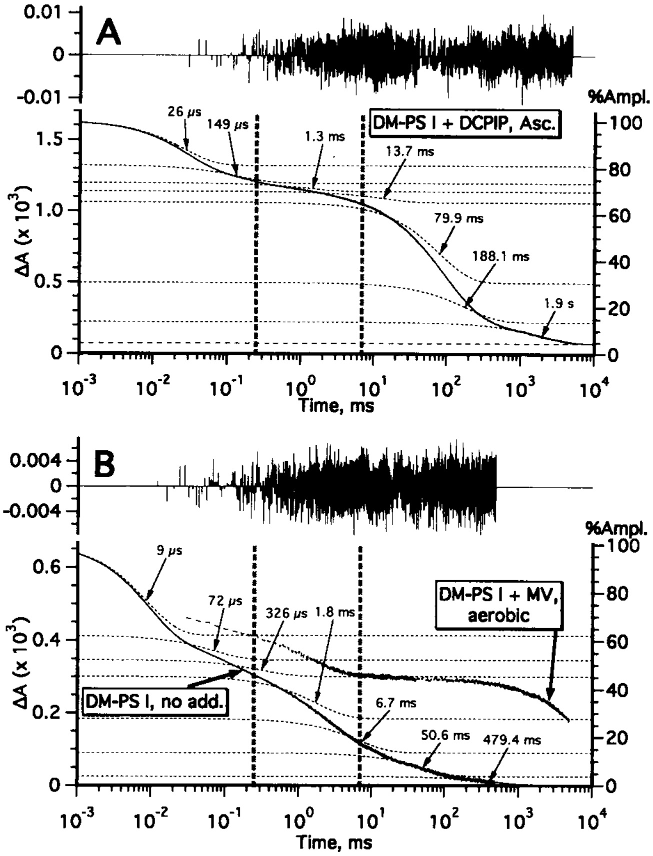

FIGURE 1 Kinetics of ΔA_{820} decay in DM-PS I preparations from *Synechocystis* sp. PCC 6803 in 25 mM Tris buffer, pH 8.3, with 0.04% DM, at chlorophyll concentration of 30 $\mu g/ml^{-1}$ (anaerobic). (*A*) in the presence of 10 mM sodium ascorbate and 4 μM DCPIP; (*B*) with no exogenous redox agents (anaerobic) and in the presence of 20 μM methyl viologen (MV, aerobic). Excitation flash (532 nm) intensity, 53 mJ; average of 12 traces acquired at 50-s intervals. Results of the multiexponential fit are displayed as the fit curve, individual exponential components, and residuals of the fit. Each individual component is plotted with vertical offset relative to the next component (with a longer lifetime) or the baseline, the offset being equal to the amplitude of the latter component. Vertical dashed bars at 250 μs and 7 ms divide the time scale into domains, where back-reactions from A_1^-, F_X^-, and $[F_A/F_B]^-$ preferentially occur.

similar to the last (not shown). The kinetic deconvolutions indicate that the fastest ΔA_{820} component that can be resolved in the DM-PS I complex has a lifetime of ~26 μs and is followed by another component with a lifetime of ~150 μs. These kinetic phases closely correspond to components with half-times of 15 μs and 110 μs (lifetimes of 22 μs and 160 μs) found for the A_1^- back-reaction in a P_{700}-A_1 core devoid of F_X, F_B, and F_A (Brettel and Golbeck, 1995). The amplitude of ΔA_{820} in the tens-of-μs time domain is higher than that found in the previous studies for DM-PS I complexes, where the contribution a component near this time domain (lifetime of 611 μs) was as low as 2% (Vassiliev et al., 1995a). However, in the previous experiments the signal-to-noise ratio of the acquisition system was higher, which resulted in higher standard errors of the fit. Furthermore, the contribution of the fastest component to the overall decay depends strongly on the excitation flash energy, and the actual energy specified in the previous paper was lower than that used in this work. As will be shown below, at high-excitation flash intensities some of the absorption change in the μs time scale can be attributed to the relaxation of a chlorophyll triplet.

The next fastest component has a lifetime of ~1.3 ms, and its contribution to the overall signal is only ~3.6%. As elaborated below, this lifetime most likely represents two unresolved components with individual lifetimes of 600 μs and 1.5 ms, and both likely correspond to back-transfer of electrons from F_X^- in this preparation (Parrett et al., 1989; Sétif and Bottin, 1989).

The major component in the DM-PS I complex has a lifetime of ~80 ms. This kinetic component comprises 35% of the total absorbance change in the averaged trace and 40% on the first flash. However, the decomposition also reveals the presence of another component with a lifetime of 12 to 14 ms, which is probably too long to be derived from the F_X^- and P_{700}^+ charge recombination (for further evidence, see below). This component, which is considerably lower in its amplitude (4–5%) than the 80-ms component, was reported earlier (Vassiliev et al., 1995a). Decomposition of the ΔA_{820} kinetics of the DM-PS I complex with no additions (Fig. 1 *B*), also reveals two components with lifetimes of ~7 ms and 50 ms. These probably correspond to the above-mentioned two components seen in the presence of reduced DCPIP, thus indicating that neither is related to direct donation from an exogenous donor to P_{700}^+. Upon addition of methyl viologen (in aerobic conditions), serving as an electron acceptor from F_A^-/F_B^-, P_{700}^+ remains stable for up to 100 ms, and the 7-ms and 50-ms phases become replaced by a slow nonexponential phase due to electron donation from the media (Fig. 1 *B*).

The slowest phases that can be resolved in the DM-PS I complex in the presence of reduced DCPIP have lifetimes of 190 ms and 1.9 s; with no additions, the slowest ΔA_{820} component has a lifetime of ~480 ms and contributes as little as 3.7% to the overall amplitude. Inasmuch as the slower components observed are negligible in DM-PS I complexes in the absence of reduced DCPIP, it is likely that they result from P_{700}^+ reduction due to exogenous chemical(s) undergoing redox reactions. Fig. 2 shows the ΔA_{820} decay in the presence of DCPIP at concentrations ranging from 4 μM to 112 μM at a relatively low excitation flash energy (~5% of that used in the experiments described above) to ensure that components in the tens-of-ms range prevail (see below). Kinetic decompositions have revealed that only the slowest component is sensitive to DCPIP concentration; Fig. 2 (*inset*) shows that its lifetime decreases from ~4 s to ~200 ms. At high DCPIP concentrations this component is difficult to separate from the 80-ms component, resulting from F_A^-/F_B^- recombination with P_{700}^+. Higher concentrations of reduced DCPIP also result in a slightly higher ΔA, most probably because of more reduction of P_{700}^+ between flashes. A similar analysis of the TX-PS I

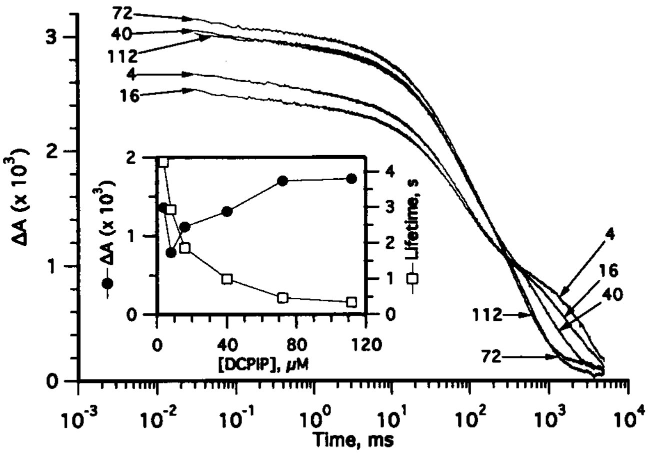

FIGURE 2 Kinetics of ΔA_{820} decay in DM-PS I preparations from *Synechocystis* sp. PCC 6803 in 25 mM Tris buffer, pH 8.3, with 0.04% DM, 10 mM sodium ascorbate, and DCPIP in concentrations from 4 µM to 112 µM, average of 16 traces. Chlorophyll concentration, 50 µg ml^{-1}. Excitation flash (532 nm) energy, 2.3 mJ. DCPIP concentration (µM) is denoted near the traces. *Inset:* the dependency of the amplitude and lifetime of the slowest component of ΔA_{820} on DCPIP concentration.

complex showed kinetics nearly identical to those of the DM-PS I complex (see below).

To determine whether the multiphase decay results from heterogeneity of the DM-PS I complex as a byproduct of the isolation procedure, we studied the ΔA_{820} kinetics in the thylakoid membranes, which serve as the starting material for the isolation of the PS I complexes. The overall shape of the back-reaction kinetics in the presence of reduced DCPIP was very similar to that of the DM-PS I complex, but the S/N was considerably lower because of the highly scattering properties of the sample. As shown in Fig. 3, the lifetimes and relative amplitudes of the major components in the isolated thylakoids are close to corresponding values for the DM-PS I complex under similar experimental conditions. However, at identical flash intensities the contribution of fast (µs to ms) phases (which are related to ^{3}Chl, as will be shown below) is considerably lower than in the DM-PS I complex at equal chlorophyll concentrations. This may be either due to the attenuation of the excitation flash energy in the scattering thylakoid suspension or to difference of energy dissipation processes in isolated and membrane-associated complexes.

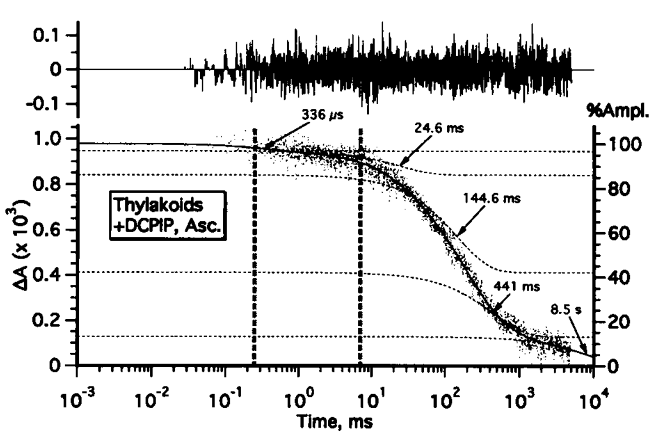

FIGURE 3 Kinetics of ΔA_{820} decay in thylakoid membranes from *Synechocystis* sp. PCC 6803 in 25 mM Tris buffer, pH 8.3, with 0.04% DM, 10 mM sodium ascorbate, and 4 µM DCPIP at chlorophyll concentration of 30 µg ml^{-1}; average of 12 traces. Excitation flash energy, 53 mJ.

Photoelectric decay phases in DM-PS I complexes

For further evidence of the intrinsic nature of back-reaction kinetics in the tens-of-ms time domain we measured the decay of the photoinduced $\Delta\psi$ across a membrane reconstituted with directionally oriented DM-PS I complexes. The conditions of the experiment were similar to the optical measurements: excitation was provided at the same wavelength, duration, and similar energy (532 nm, 15 ns, 40 mJ). The concentrations of external electron donors (DCPIP, sodium ascorbate) were identical, but the pH was 10.0 rather than 8.3. Subsequent optical experiments showed that the ΔA_{820} kinetics were the same at both pH values (not shown).

Consistent with previous results on PS I in *Anacystis nidulans* (Mamedov et al., 1995), flash excitation leads to generation of a membrane potential with negative polarity inside the proteoliposome at times faster than the time resolution of the instrument (200 ns). As shown in Fig. 4, the kinetics of the $\Delta\psi$ decay of DM-PS I complexes measured in the presence of reduced DCPIP show two major decay components in the tens-of-ms time domain with lifetimes of 13 and 81 ms, with relative amplitudes (9% and 27%), which are similar to the major components of the ΔA_{820} decay (Fig. 1 *A*). Hence, these kinetic phases are assigned to $[F_A/F_B]^-$ back-reaction, thus confirming the biphasic nature of the P_{700}^+ $[F_A/F_B]^-$ charge recombination

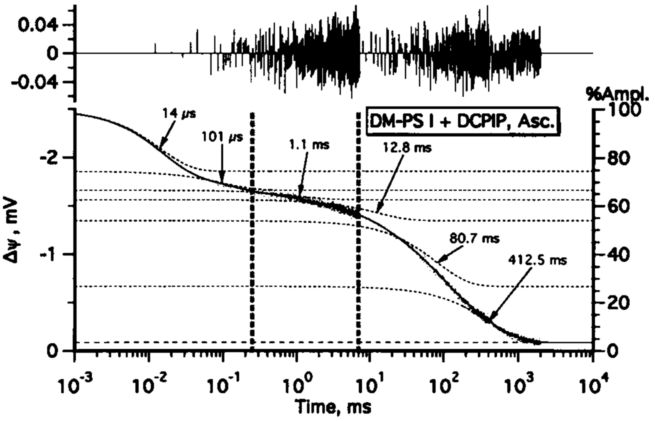

FIGURE 4 Decay kinetics of the flash-induced photoelectric response ($\Delta\psi$) of the proteoliposomes with DM-PS I complex from *Synechocystis* sp. PCC 6803; a single flash acquisition. Excitation flash energy, 40 mJ. The reaction medium is: 200 mM glycine buffer, pH 10, with 10 mM sodium ascorbate and 4 µM DCPIP. Chlorophyll concentration, 1.8 µg ml^{-1}.

using two independent experimental techniques. The slower component has a lifetime of ~413 ms and contributes ~23% to the overall decay. The faster phases resolved in this preparation have lifetimes of ~14 μs, 101 μs, and 1.1 ms; they make up, respectively, 25%, 7.9%, and 4% of the overall signal. Unlike the ΔA_{820} kinetics, ^{3}Chl decay should not lead to a photovoltage because no vectoral charge separation or recombination event is involved. Because decreasing the excitation energy down to 1 mJ resulted in about the same extent of decrease of the amplitudes of the relevant components, including the 14-μs phase, and as it is not observed in the case of liposomes with no PS I complexes incorporated, this phase is related to real processes in the PS I complex and not to some electric artifact. However, it is conceivable that some PS I complexes incorporated into membrane could have lost the F_X cluster during sonication, which should lead to 14-μs back-reaction from A_1^-. Also, if the distance between P_{700} and the terminal electron acceptor was increased due to conformational changes in the PS I complex accompanying forward electron transfer, then electrostriction of the complex manifest as another decay phase could take place within times shorter than the back-reaction.

It should be noted that an electrogenic response of about the same magnitude can be measured in the PS I complex even in the absence of exogenous electron donors (Semenov et al., manuscript in preparation), a result consistent with an observation by Sigfridsson et al. (1995). This implies that P_{700} is present in the reduced state upon incorporation of PS I complex into liposomes. The lifetimes and amplitudes of components resolved in these conditions were essentially the same; however, the slowest phase (lifetime of 413 ms) which might be attributed to the passive discharge across the membrane, was not detected in the absence of an exogenous electron donor.

Flash saturation dependency of ΔA_{820} kinetics

Inasmuch as the quantum yield of charge separation is ~1.0 in PS I, the terminal electron acceptors F_A and F_B should be efficiently photoreduced in the PS I complex and there should be no evidence for back-reactions from earlier acceptors. Therefore, appearance of μs phases can be related to either the A_1^- back-reaction in the fraction of damaged centers, which do not reduce F_X and/or F_A/F_B, or to the decay of the ^{3}Chl, which takes place in the μs-to-ms time scale (Sétif et al., 1981). Regarding ^{3}Chl we suggest two possibilities: a) a $^3P_{700}$ formed in a recombination reaction of P_{700}^+ with a photoreduced acceptor of PS I, and b) a PS I antenna ^{3}Chl formed upon flash excitation as a result of deactivation of S_1-state Chl molecules incapable of energy transfer to the reaction center (because the latter is in the closed state). The second mechanism is quite feasible, and perhaps likely, given the nonspecific excitation of antenna chlorophyll molecules with a Nd-YAG laser flash at 532 nm (Nuijs et al., 1986; Shuvalov et al., 1986).

We monitored the ΔA_{820} kinetics in DM-PS I complexes at different levels of excitation flash energies to investigate whether the faster kinetic phases appear at all energies. Fig. 5 *A* shows the traces acquired without a 300-kHz high-frequency roll-off filter at different excitation flash intensities in a DM-PS I complex in the presence of reduced DCPIP. With the data acquisition setup used in this experiment no strict discrimination between components decaying slower than tens-of-ms were made by the fitting program, and they appear as a single component with a lifetime of 115–120 ms and a baseline. We assume that the components with lifetimes of ~10-20 ms and 80–100 ms (F_A^-/F_B^- back-reaction) and slower (P_{700}^+ reduction from slow exogenic donors) represent the decay of a DM-PS I complex with normally functioning terminal acceptors because these phases are eliminated upon physical removal of PsaC or upon chemical reduction of F_A/F_B. Thus, we have analyzed the flash energy dependency of the sum of amplitudes of these components rather than their individual amplitudes. Taking into consideration that the components with ms- and sub-ms lifetimes (i.e., those related to F_X^- back-reaction) are of low amplitude and sometimes not well resolved in the isolated DM-PS I complexes (yielding just one component with lifetime ~1 ms) we plotted the flash energy dependence of the sum of these two components. As seen from Fig. 5 *C*, the kinetics in tens-of-ms time domain becomes completely saturated at flash intensities of 10 mJ, and there are almost no μs-to-ms kinetics at lower flash levels. The fastest components with lifetimes of ~10 μs and 100 μs appear only at flash intensities >10 mJ, and their flash intensity dependency is uniquely different from that of the other components. The ms-component was resolved at all

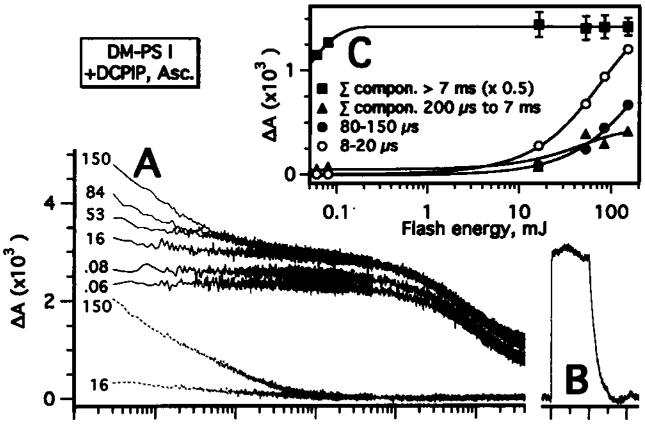

FIGURE 5 (*A*) Kinetics of ΔA_{820} decay in DM-PS I preparations from *Synechocystis* sp. PCC 6803 with (*dotted traces*) and without (*solid line traces*) background illumination at 710 nm. Laser flash excitation was provided at different energy values, which are denoted (in mJ) near the traces. (*B*) Steady-state kinetics of ΔA_{820}. (*C*) The dependency of amplitudes of ΔA_{820} decay on the excitation flash energy (the overall amplitude of components with lifetimes >7 ms is scaled by multiplying by a factor of 0.5). Samples were suspended in 25 mM Tris buffer, pH 8.3, with 0.04% DM, 10 mM sodium ascorbate, and 4 μM DCPIP at chlorophyll concentration of 50 μg ml^{-1}.

flash energies used in this experiment; however, its contribution at high energies is lower than for the μs-components.

One way to discriminate between the fast components arising from the back-reactions and those related to ^{3}Chl is to compare the levels of flash-induced P_{700} photoreduction with steady-state levels attained at more selective excitation of P_{700} in the far-red. We have monitored the ΔA_{820} decay kinetics at a highest-time resolution at two flash energy levels (16 mJ and 150 mJ), both with and without a saturating background illumination. As seen from Fig. 5, *A* and *B*, the steady-state absorbance change attained using continuous far-red light (710 nm) is close to the plateau of the flash-induced signal at 16 mJ energy, which is dominated by tens-of-ms components. Applying 16-mJ energy flashes to the DM-PS I with simultaneous background illumination leads to only a minor absorbance increase relative to the background-light-induced level. At 150-mJ flash excitation with background illumination, however, there is a fast ΔA_{820} decay occurring in the μs-to-ms time domain, which indicates the participation of ^{3}Chl in the decay kinetics.

ΔA_{820} kinetics in F_B-less TX-PS I complexes

The kinetics of ΔA_{820} were next determined in TX-PS I preparations in which electron transport involves iron-sulfur cluster F_A but not F_B. We measured the ΔA_{820} decay in the μs-to-s time domain in the TX-PS I complex after the F_B cluster was selectively destroyed by $HgCl_2$ (Kojima et al., 1987). To confirm the EPR evidence (Jung et al., 1995) for the destruction of the F_B cluster, we characterized this very same sample using a standard multiple-flash protocol described elsewhere (Bottin et al., 1987; Sauer et al., 1978) at room temperature in the presence of a fast donor to P_{700}^+ (reduced PMS) at pH 6.5 in aerobic conditions. In the untreated PS I complex, reduction of P_{700}^+ by reduced PMS overrides the faster reaction(s) involving F_X^- and/or A_1^- only before the second flash, when the electrons are stabilized on both F_A and F_B. After photoreduction of F_A and F_B the faster back-reactions from F_X^- and A_1^- with lifetimes shorter than 1 ms become dominant. Therefore, the kinetics for the second flash are similar to those for the first and the kinetics for the fourth flash are close to the third (see below). In the F_B-less sample a 3-ms component due to electron donation from reduced PMS to P_{700}^+ was detected only after the first flash, which indicates that only one of the two terminal clusters is available for photoreduction (data not shown; see Yu et al., 1996; also Sakurai et al., 1991).

The ΔA_{820} kinetics of the $HgCl_2$-treated sample measured in the presence of reduced DCPIP retain all major decay components observed in the TX-PS I control sample, with relatively consistent lifetimes (Fig. 6). However, the sample shows an increase in the amplitudes of the faster components with lifetimes of 29 μs, 269 μs, and 1.4 ms at the expense of the slower components. Also, the components assigned to the back-reactions of F_A and/or F_B are significantly faster (11 ms vs. 16.6 ms and 38 ms vs. 65 ms) than in the TX-PS I control. Comparison of the decomposition amplitudes and kinetics of the control and $HgCl_2$-treated samples of this batch and other batches (not shown) in the 10–200 ms time domain does not reveal any preferential changes of a particular component's parameters, which would allow one to implicate a specific kinetic phase to the destroyed F_B.

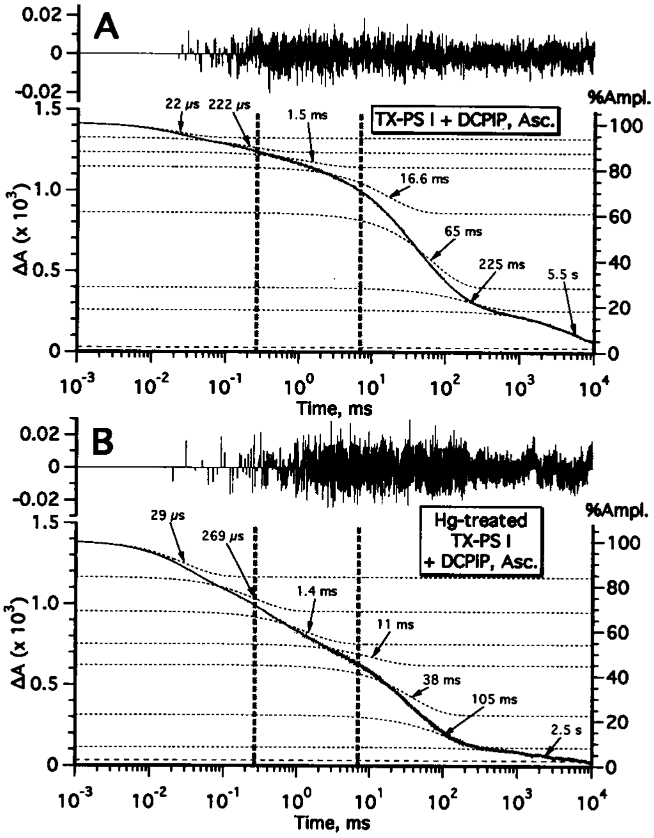

FIGURE 6 Kinetics of ΔA_{820} decay in untreated (*A*) and $HgCl_2$-treated (*B*) TX-PS I complexes from *Synechococcus* sp. PCC 6301 in 25 mM Tris buffer, pH 8.3, with 0.04% Triton X-100, 10 mM sodium ascorbate, and 4 μM DCPIP at chlorophyll concentration of 30 μg ml^{-1}; average of 12 traces. Excitation flash energy, 53 mJ.

PS I complexes with reduced F_A and F_B clusters and P_{700}-F_X cores

ΔA_{820} decay phases

We next studied the kinetics of ΔA_{820} in PS I preparations in which electron transport terminates at iron sulfur cluster F_X. Its recombination with P_{700}^+ becomes the dominant back-reaction pathway when the PS I complex is physically devoid of the PsaC protein or when F_A and F_B are chemically reduced. We compared the ΔA_{820} kinetics in three preparations: a) a DM-PS I complex with F_A and F_B clusters reduced by sodium dithionite in darkness at pH 10.0; b) a DM-PS I complex with F_A and F_B clusters photoreduced by two preilluminating flashes in the presence of PMS and sodium dithionite in at pH 6.3; and c) a P_{700}-F_X core isolated from a DM-PS I complex by urea treatment.

Sauer and colleagues (1977) showed that in the presence of dithionite a back-reaction of an acceptor preceding F_A and F_B gives rise to a 250-μs component now recognized as the back-reaction from F_X. Sétif and Bottin (1989) observed much faster kinetics upon strong continuous illumination in the presence of dithionite, conditions under which the double reduction of A_1 as well as the photoreduction of F_X has been shown to occur. After trial experiments with different dithionite concentrations we used a concentration of 100 mM at pH 10.0, which is sufficient to remove >90% of the tens-of-ms component(s) (Fig. 7). Comparing the single flash-induced trace with that resulting from eight averages, we found virtually no change in ΔA_{820} kinetics in the course of consecutive excitations at 50-s intervals (not shown). The multiexponential fit of kinetics acquired at saturating flash energy (16 mJ) yields the major component with a lifetime of 448 μs (56%) which is assigned to the F_X^- back-reaction. This component is followed by a minor 1.5-ms component (~10%) and is preceded by components with a lifetime of 8 μs (30%). To investigate the relevance of the latter component to decay of the ^{3}Chl, we monitored the ΔA_{820} kinetics at different excitation flash energies (Fig. 7 *A*). As seen from the decomposition results (Fig. 7 *C*), increase of the flash energy >4 mJ gives a strong rise to the contribution of this component. At highest flash energies tested (53 mJ and 150 mJ) another component with a lifetime of 50–80 μs is revealed in the decomposition.

The kinetics of the DM-PS I complex with F_A and F_B clusters photoreduced by two preilluminating flashes in the presence of PMS and sodium dithionite at pH 6.3 are essentially the same as those of a complex with chemically prereduced clusters. Fig. 8 *A* shows the traces acquired in these conditions with a total of one, two, three, and four flashes in a sequence. The results of a global 3-exponential fit of the data set are shown in Fig. 8 *A* (flash #1 only) and Fig. 8 *B* (flash #3). As seen from comparing these two decomposition sets, preillumination with two flashes leads to significant elimination of the 2.63-ms component, which

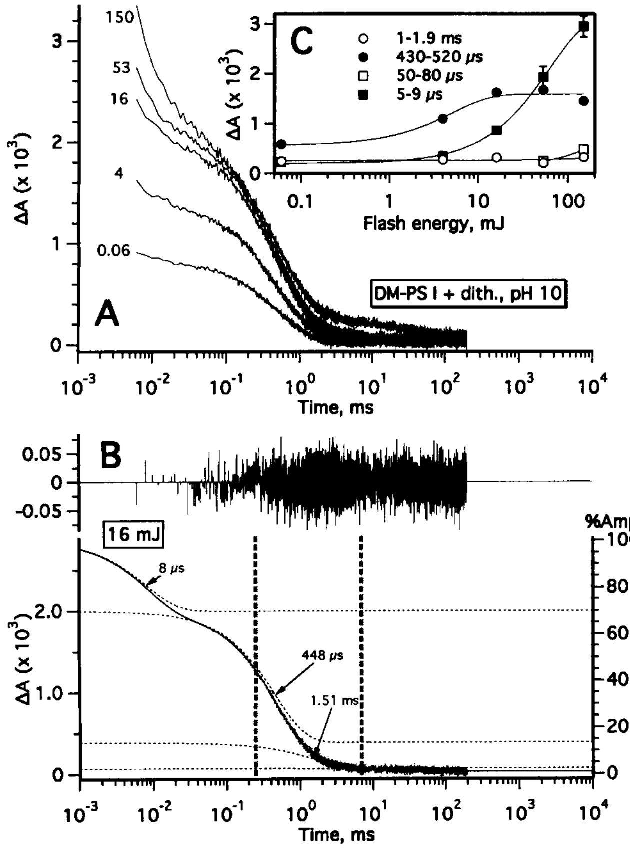

FIGURE 7 (*A*) Kinetics of ΔA_{820} decay in DM-PS I preparation from *Synechocystis* sp. PCC 6803 in 100 mM glycine buffer, pH 10, with 0.04% DM and 100 mM sodium dithionite at chlorophyll concentration of 50 μg ml^{-1}; average of 16 traces. Laser flash excitation was provided at different energy values, which are denoted (in mJ) near the traces. (*B*) Multiexponential fit of the kinetics measured at 16 mJ excitation. (*C*) The dependency of amplitudes of ΔA_{820} decay on the excitation flash energy.

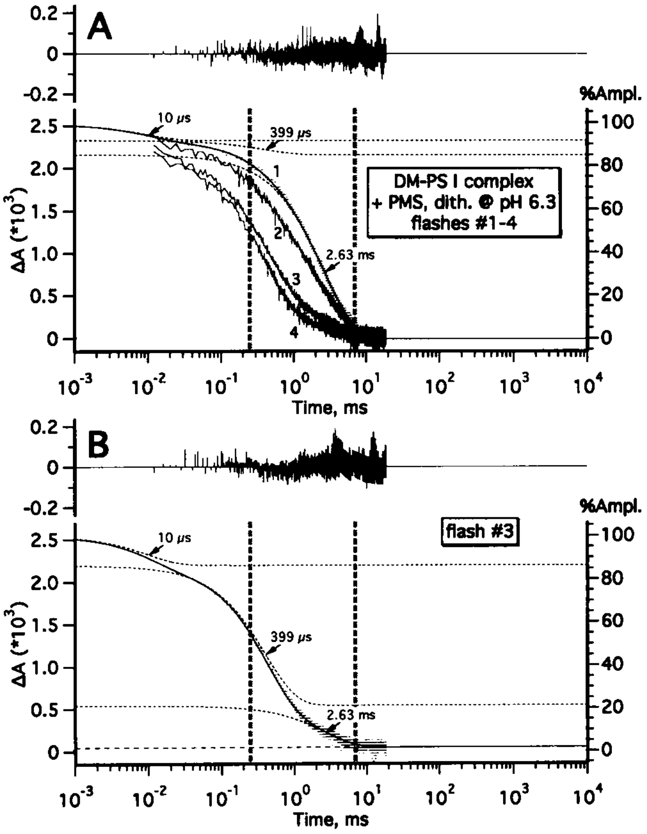

FIGURE 8 Kinetics of ΔA_{820} decay in DM-PS I complex from *Synechocystis* sp. PCC 6803 at chlorophyll concentration of 50 μg ml^{-1} upon excitation Nd-YAG laser flash (16 mJ) preceded with Xenon lamp flashes (see Materials and Methods). (*A*) Kinetics with a total of 1–4 flashes (the numbers of flashes are indicated near the curves), and multiexponential fit of the kinetics with no preilluminating flashes. (*B*) Multiexponential fit of the kinetics with flashes. The reaction media (aerobic) is: 25 mM MES buffer, pH 6.3, with 0.02% Triton β-DM, 10 μM PMS, and 2 mM sodium dithionite. The samples were dark-adapted for 4 min after addition of freshly prepared mediators.

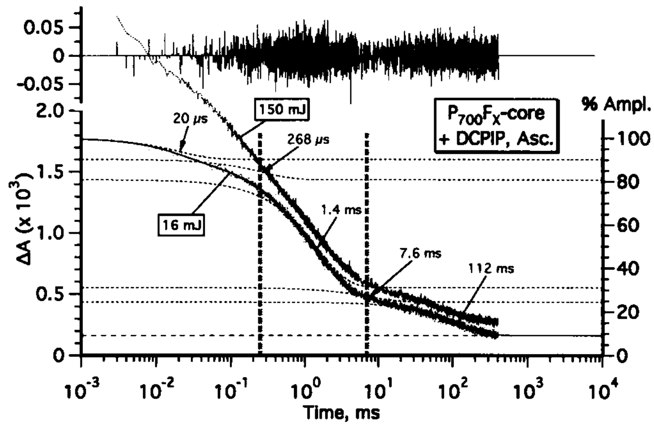

FIGURE 9 Kinetics of ΔA_{820} decay in P_{700}-F_X core preparation from *Synechocystis* sp. PCC 6803 in 25 mM Tris buffer, pH 8.3, with 0.04% DM, at chlorophyll concentration of 50 μg ml^{-1} in the presence of 10 mM sodium ascorbate and 4 μM DCPIP. The traces were obtained at flash excitation energies of 16 mJ and 150 mJ; the multiexponential fit results are presented for 16 mJ only.

results from electron donation from reduced PMS to P_{700}^{+}. The major component on the third flash has a lifetime of 399 μs, and it makes up >60% of the overall ΔA_{820}. (Fig. 8 *B*). Because the PMS-component of ΔA_{820} is still present, however, with two preilluminating flashes (2.63 ms, ~20%), it is most likely that this exogenous electron donor overrides reduction of P_{700}^{+} from F_X^{-} in a certain fraction of centers. Therefore, the component with a close lifetime of ~1.5 ms observed upon chemical reduction of the terminal iron-sulfur clusters (Fig. 7 *A*) is overridden by the forward donation from reduced PMS. A μs-time scale component can be also resolved both with and without preilluminating flashes. It has a lifetime of 10 μs and contributes ~10% with no preilluminating flashes, and ~15% with two preilluminating flashes (Fig. 8 *A* and *B*).

The multiexponential decomposition analysis of ΔA_{820} kinetics of an urea-prepared P_{700}-F_X core is shown in (Fig. 9). At 16 mJ excitation flash energy the ΔA_{820} decay has the major component with a lifetime of 1.4 ms (~50%), which is attributed to the back-reaction of F_X^{-} with P_{700}^{+}. The contributions of faster components with lifetimes of 20 μs and 268 μs are each ~10%. The contribution of components in the tens-of-μs time domain is selectively increased at higher flash energies (compare with trace at 150 mJ, Fig. 9). Slower decay components with lifetimes of 7.6 ms and 112 ms make up, along with the baseline, ~30% of the total absorption change. These components obviously correspond to a fraction of centers still possessing the PsaC protein.

Photoelectric decay phases

The photoelectric decay kinetics of the P_{700}-F_X core isolated from the TX-PS I complex are similar to the above-mentioned ΔA_{820} kinetics of the P_{700}-F_X core from DM-PS I; there are three resolved phases with lifetimes of 15 μs, 261 μs, and 1.4 ms (Fig. 10 *A*) The lifetimes of the photoelectric decay measured in DM-PS I in the presence of dithionite are very close to those measured optically at ΔA_{820} (Fig. 10 *B*), with the 1-ms component being the prominent kinetic phase (~38%). The differences in the amplitudes relative to the amplitudes of the ΔA_{820} decay may be explained by relevance of the photovoltage amplitudes to dielectrically weighed, rather than physical, distances between the electron transport chain components (Leibl et al., 1995). The presence of ~30% of fast phase with a lifetime of ~15 μs can be explained, as in the case of the integral complex (see above), by lack of photochemically active F_X in a fraction of centers and/or the electrostriction effect.

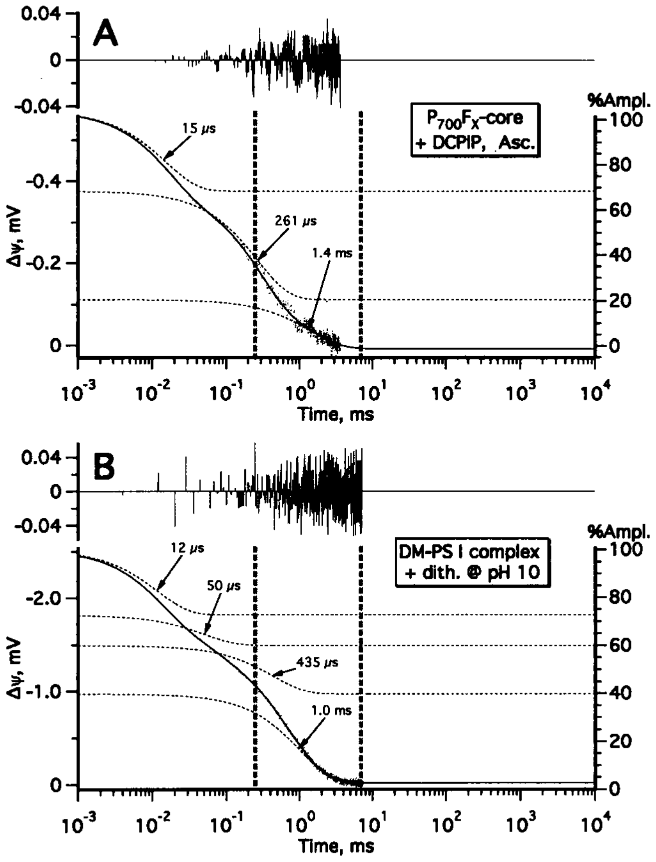

FIGURE 10 Decay kinetics of the flash-induced photoelectric response ($\Delta\psi$) of the proteoliposomes with P_{700}-F_X complex from *Synechococcus* sp. PCC 6301 in 200 mM glycine buffer, pH 10, with 10 mM sodium ascorbate and 4 μM DCPIP (*A*) and proteoliposomes with DM-PS I complex from *Synechocystis* sp. PCC 6803 in 200 mM glycine buffer, pH 10, with 100 mM sodium dithionite (*B*). Chlorophyll concentration, 1.8 μg ml^{-1}, excitation flash energy, 40 mJ.

ΔA_{820} decay phases in P700-A_1 cores

To verify the assignments of the ΔA_{820} phases made in the P_{700}-F_X cores we used the same experimental setup to measure the decay kinetics in a P_{700}-A_1 core devoid of the F_X, F_A, and F_B clusters. We have found the ΔA_{820} kinetics of this preparation to be strongly dependent on the presence of oxygen (not shown): in anaerobic conditions the kinetics comprised a considerable amount of a component decaying with a lifetime of ~600 μs, but subsequent air saturation of the same sample resulted in dramatically faster kinetics. On the other hand, this oxygen effect was much less pronounced in a P_{700}-F_X core, and mostly occurred in the time domain up to 50 μs; on a longer time scale the kinetics of the aerobic and anaerobic samples were similar. This effect may be rationalized by assuming that destruction of the interpolypeptide F_X cluster changes the interaction of chlorophyll molecules within the PsaA/PsaB heterodimer in a manner that increases the yield and the lifetimes of ^{3}Chl states in the absence of oxygen. The latter acts as a quencher of ^{3}Chl (Mathis and Sétif, 1981).

Because the decay of ^{3}Chl and recombination of the $P_{700}^+A_1^-$ pair take place in the same time domain, it is particularly important to separate these two processes. Fig. 11 *A* shows the ΔA_{820} kinetics measured at different excitation flash energies. Unlike the case of a DM-PS I complex (Figs. 5 and 7) or a P_{700}-F_X core (Fig. 9), there is no obvious saturation of a particular component seen in the case of a P_{700}-A_1 core. Moreover, the approach used to determine the amount of photoxidized P_{700}^+ upon steady-state excitation at 710 nm used for the DM-PS I complex (Fig. 5) cannot be applied in the case of a P_{700}-A_1 core, as the ΔA_{820} steady-state signal is not saturated at available excitation energies of 20 mW from the titanium-sapphire laser. We attempted to reach the maximum oxidation of P_{700} by applying the steady-state illumination in the presence of ferricyanide at pH 6.3, and monitor the ^{3}Chl decay at different excitation flash energies from the Nd-YAG laser. As seen from Fig. 11 *A*, a strong ΔA_{820} signal can be measured in these conditions at 150 mJ flash energy (*upper dashed trace*), but the ΔA_{820} appearing at 3 mJ (*bottom dashed trace*) is relatively weak in comparison with the one monitored at 3 mJ flash energy in reducing conditions (*solid line*). We have made a muliexponential fit of this weak ^{3}Chl-decay signal and subtracted it from the reducing-conditions kinetics. The fit of the resulting trace shown in Fig. 11 *B* yields two components with lifetimes of 11 μs and 132 μs at amplitude ratio 2.67, values that correspond to those reported in the previous study on the P_{700}-A_1 preparation (Brettel and Golbeck, 1995). The remaining 16% of the decay signal amplitude is approximated by a baseline, accounting for slower components. The analysis of the original decay kinetics at 3 mJ without subtraction of the ^{3}Chl signal yielded similar results, with a slightly higher contribution of the fast component (not shown).

DISCUSSION

Our studies of the kinetics of ΔA_{820} and $\Delta\psi$ can be categorized in two discrete classes: *PS I complex-type* (isolated thylakoids, DM-PS I complex, and TX-PS I complex), with most of the decay occurring in the tens-of-ms time domain, and *PS I core-type* (P_{700}-F_X core, PS I complexes with chemically reduced F_A/F_B, and P_{700}-A_1 core) with most of the decay occurring in the μs-to-ms time domain (see summary in Table 1). Using values obtained from studies of biochemically resolved preparations with known functioning electron acceptors, any decrease in the forward electron transfer efficiency in PS I preparations should lead to kinetics which can then be decomposed and assigned to the appropriate electron acceptor(s). A discussion of the identification of a kinetic lifetime with a given electron transfer component follows.

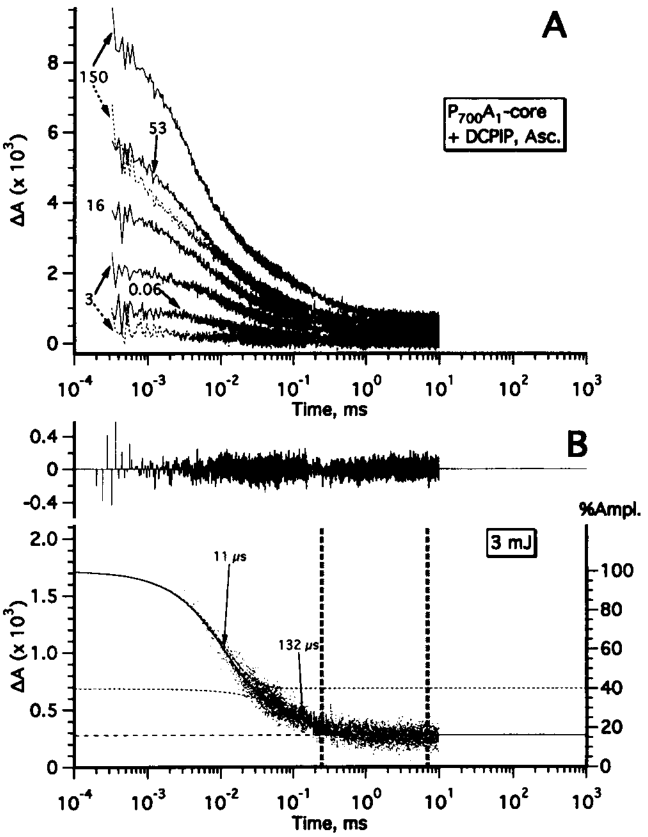

FIGURE 11 (*A*) Kinetics of ΔA_{820} decay in P_{700}-F_X and P_{700}-A_1 core preparations from *Synechococcus* sp. PCC 6301 in 25 mM Tris buffer, pH 8.3 (aerobic) with 0.04% DM, 10 mM sodium ascorbate, and 4 μM DCPIP at chlorophyll concentration of 50 μg ml^{-1}; average of 40 traces (no 300-kHz roll-off filter). Laser flash excitation was provided at different energy values, which are denoted (in mJ) near the traces. Dashed lines denote traces measured in the presence of 40 mM ferricyanide at pH 6.3 and background illumination. (*B*) multiexponential analysis of kinetics of ΔA_{820} decay in P_{700}-A_1 core preparation at excitation flash energy of 3 mJ, with prior subtraction of the multiexponential fit of the signal monitored at this flash intensity in the presence of ferricyanide at pH 6.3 and background illumination. Note that the span of the time scale in this figure differs from the others.

Back-reactions of F_A and F_B

A detailed analysis of the ΔA_{820} kinetics showed that recombination of $[F_A/F_B]^-$ with P_{700}^+ occurs as two exponen-

TABLE 1 Assignments of kinetic components of P_{700}^{+} reduction in different PS I preparations. The table represents the values derived in typical ΔA_{820} measurements. The values may vary slightly depending on the type of preparation and/or for electric potential kinetics (see text for details). The ^{3}Chl decay data are also included for comparison

Mechanism	Major component(s), lifetime(s), and ratio of amplitudes	Sample and conditions for monitoring
P_{700}^{+} $[F_A/F_B]^-$ recombination	10 ms; 80 ms (1:4)	Integral PS I complex in the presence of reduced DCPIP at pH 8.3
P_{700}^{+} F_x^- recombination	450 μs; 1.5 ms (5:1)	Integral PS I with F_A and F_B reduced by dithionite at pH 10, or preillumination with two flashes in the presence of reduced PMS at pH 6.3
	270 μs; 1.5 ms (1:5)	P_{700}-F_x core in the presence of reduced DCPIP at pH 8.3
P_{700}^{+} A_1^- recombination	10 μs; 130 μs (2.7:1)	P_{700}-A_1 core in the presence of reduced DCPIP at pH 8.3 in aerobic conditions
Direct donation to P_{700}^{+} from reduced DCPIP (4 μM)	200 ms; 2 s (ca.1:1)	Integral PS I complex in the presence of reduced DCPIP at pH 8.3
Direct donation to P_{700}^{+} from reduced PMS (10 μM)	2.6 ms	Integral PS I complex in the presence of reduced PMS at pH 6.3
Antenna ^{3}Chl decay	10 μs	In all above preparations at oversaturating excitation flash energies (>20 mJ)

tial components with lifetimes of 10–20 ms (the minor kinetic phase) and 80–100 ms (the major kinetic phase). Inasmuch as the two components were resolved in isolated thylakoids, in DM-PS I complexes from *Synechocystis* sp. PCC 6803 irrespective of reduced DCPIP, and in TX-PS I complexes from *Synechococcus* sp. PCC 6301, the presence of these two phases is not related to an artifact arising from the isolation procedure. Previous analysis of the ΔA_{820} kinetics in Triton X-100-isolated PS I complexes showed that the major contribution was derived from a component with a half-time of ~30 ms (lifetime, ~48 ms), which was subsequently assigned to the recombination of F_A^- and/or F_B^- with P_{700}^{+} (Sauer et al., 1978). This is faster than the value of 80 ms in the present work, leading us to suggest that the component with a previously reported half-time of 30 ms is probably an unresolved mixture of the 12-ms and 80-ms components.

The kinetics on each excitation flash are essentially the same, which indicates that the multiphase pattern of the averaged kinetics is not an artificial overlapping of traces differing in their individual kinetics. An analysis of relaxation kinetics of the photoinduced $\Delta\psi$ in DM-PS I complexes incorporated into a phospholipid bilayer membrane serves as further evidence for the intrinsic biexponential kinetics of the recombination reaction between $[F_A/F_B]^-$ and P_{700}^{+}.

However, the 10- to 20-ms and 80- to 100-ms components cannot be assigned uniquely to the individual acceptors F_A and F_B because these two decay components are also present in a $HgCl_2$-treated complex that lacks F_B. The 15 K EPR spectrum of this particular sample shows no more than 5% of the control amount of photoactive F_B, whereas photoreduction of F_A is unaffected at low temperature (Jung et al., 1995). The overall amplitude of these two above-mentioned ΔA_{820} components in the $HgCl_2$-treated sample is decreased at the expense of faster components derived from F_X^- (1.4-ms and, most likely, 269-ms components) and A_1^- (contribution to the 29-ms component). Whereas a higher yield of back-reaction from F_X^- to P_{700}^{+} should indicate a decreased quantum efficiency of photoreduction of F_A in the absence of F_B, the increase of the amplitudes in the 29-μs component is probably a side effect of $HgCl_2$ treatment on F_X in a minority of centers, which could not be precisely quantitated by EPR (Jung et al., 1995). Hence, if electron transfer is serial through the terminal acceptors, then these results suggest that F_B plays a hitherto-undisclosed role in maintaining a high efficiency of forward electron transfer beyond A_1 and F_X through F_A to ferredoxin (or flavodoxin) in PS I. Alternatively, if electron transfer is parallel, then the loss of amplitude represents that portion of electron transfer through the F_B that is lost.

Given the relatively similar reduction potentials for F_A (−530 mV) and F_B (−580 mV) and the finding that F_A can be photoreduced at low temperatures in the absence of F_B, we suggest that either a) recombination of both F_A^- and F_B^- with P_{700}^{+} results in the biphasic kinetics with lifetimes of ~10 and 80 ms, b) only F_A^- can reduce P_{700}^{+} in a back-reaction, or c) rapid electron equilibration between F_A and F_B eliminates the distinction between the two electron acceptors in terms of individual contribution to the kinetics. The presence of these two decay components could be explained by the presence of different conformational states in the PS I complex. Multiphase exponential kinetics were observed previously for back-reactions of primary quinone, Q_A, in Photosystem II (Gerken et al., 1989) and both primary and secondary quinones (Q_A and Q_B) in reaction centers of *Rhodopseudomonas viridis* (Gao et al., 1991; Baciou and Sebban, 1995). In all instances, it was suggested that deviation from monoexponential kinetics resulted from distribution of different structural states of the reaction center protein(s). Based on studies of the pH dependencies in the bacterial preparations (Gao et al., 1991) the biexponential pattern was attributed to the existence of two reaction center conformers differing in their protonation states. However, at least in the case of DM-PS I complex from *Synechocystis* sp. PCC 6803, our analysis of pH dependencies of the ΔA_{820} decay kinetics in the range from pH 4.5 to pH 10 did not reveal any significant differences in the parameters of the components relevant to the F_X and F_A/F_B back-reactions (data not shown).

In both PS I complexes and thylakoid membranes the major phases arising from back-reactions of $[F_A/F_B]^-$ to P^+_{700} are followed by one or two slower kinetic phases. The components decaying on the hundreds-of-ms to seconds time scale are usually attributed to the reduction of P^+_{700} from exogenous components of the media (Lüneberg et al., 1994; Sigfridsson et al., 1995). The phase with a lifetime of ~2-4 s represents direct donation from reduced DCPIP to P^+_{700}, as follows from the dependence of its lifetime and amplitude on DCPIP concentration. This component usually makes up from 10 to 20% of the total ΔA_{820} amplitude. A component with a lifetime varying from 200 to 400 ms could be resolved in the isolated complex, but in thylakoid membranes this phase could not be observed, and only three components (with lifetimes of ~10-20 ms, 80–120 ms, and 2–4 s) were resolved in the ms-to-s time domain. The relative contribution of the 200- to 400-ms component was highly variable from sample to sample, but given that it is almost not present in both electrogenic and optical measurements without reduced DCPIP, it is most likely that this phase, along with the 2- to 4-s phase, represents direct donation to P^+_{700} from this external donor.

Back-reactions of F_X and A_1

The tens-of-ms components arising due to F_A and F_B back-reactions and P^+_{700} reduction from slow exogenous donors are eliminated if the PsaC protein is missing due to chaotrope treatment, or if the F_A and F_B clusters are chemically or photochemically reduced. The contribution of these components is also decreased in mutants with ligand substitutions at the F_A and F_B sites (Yu et al., 1996). Thus, the sum of amplitudes of kinetic phases with lifetimes >7-10 ms can be used as a robust estimate of the efficiency of electron transfer to terminal iron-sulfur clusters. In above cases, the ΔA_{820} decays essentially on a milliseconds time scale. Summarizing the ΔA_{820} and electric potential decay data acquired in the above conditions and taking into account the results of this and previous work (Brettel and Golbeck, 1995) that the ΔA_{820} decay in the P_{700}-A_1 core occurs with lifetimes of ~10 μs and 100 μs, we can assign slower components arising in these conditions to back-reaction between F^-_X and P^+_{700}.

In the case of a PS I complex with chemically or photochemically reduced terminal iron-sulfur clusters, the ΔA_{820} component with a lifetime of ~400-450 μs (>50% contribution) can be definitely ascribed to the back-reaction between F^-_X and P^+_{700}. In PS I complex with chemically reduced terminal clusters there is also a slower component (1.5 ms), which makes up ~15% of the total amplitude; in the experiment with photochemical reduction of F_A and F_B, this component is obviously overlapped by the phase arising from direct electron donation from PMS-H_2 in a fraction of centers (a 2.63-ms component, 20% of amplitude). There is also a component with a lifetime of ~8-10 μs present in both conditions (see below). In isolated P_{700}-F_X cores, the kinetics are more complex due to the obvious heterogeneity of the sample. However, if we exclude the 7.6-ms and 112-ms components (plus baseline) accounting for a fraction still possessing the PsaC protein, then the remaining kinetics should consist of the major 1.4-ms phase (72%) and two minor phases with lifetimes of 20 μs and 268 μs (10% each).

It should be noted that in the three cases above a fast component with a lifetime of ~10-20 μs exists. If we rule out the participation of ^{3}Chl at low flash excitation energies, then the appearance of this component should be related to a back-reaction in the PS I reaction center. We consider two possible mechanisms for this back-reaction: a) electron transfer from F^-_X via A_1 to P^+_{700}, occurring due to redox equilibrium between A_1 and F_X (Sétif and Brettel, 1993), or b) recombination between P^+_{700} and A^-_1 in a fraction of centers with blocked electron transfer to F_X. Regarding the first possibility, the single electron transfer in the P_{700}-F_X core can be modeled by a scheme analyzed previously for bacterial reaction centers containing photoactive primary and secondary quinone acceptors in the absence of fast donation to the pigment (Rubin and Shinkarev, 1984; Shinkarev and Wraight, 1993). This model should be valid in the case of an isolated P_{700}-F_X core in the presence of reduced DCPIP, which donates electrons to P^+_{700} ~10^3 times slower than F^-_X:

$$\begin{tikzcd} P^1_{700}A^0_1F^0_X \arrow[r, shift left, "k_{PA}"] & P^0_{700}A^1_1F^0_X \arrow[l, shift left, "k_{AP}"] \arrow[r, shift left, "k_{AX}"] & P^0_{700}A^0_1F^1_X \arrow[l, shift left, "k_{XA}"] \arrow[ll, bend left, "k_{XP}"'] \end{tikzcd}$$

where 0 stands for oxidized and 1 for reduced electron carrier. This model accounts for two possible routes of electron transfer from F^-_X, potentially yielding two exponential components of P^+_{700} decay determined in the experiment: a) direct recombination with P^+_{700} (rate constant k_{XP}), and b) return of electron to A_1 (rate constant k_{AX}) with subsequent recombination of the $P^+_{700}A^-_1$ pair (rate constant k_{PA}).

Taking into account that the rate constant k_s of the main (slower) component of ΔA_{820} decay is at least an order of magnitude lower than both k_{AP} and rate constant of the fast component (k_f, which is higher than k_{PA}), the contribution of the fast component can be calculated according to Rubin and Shinkarev (1984), as follows:

$$R_f = \frac{k_{AP} - k_s}{k_f - k_s} \leq \frac{k_{AP}}{k_f} \approx \frac{k_{AP}}{k_{AX} + k_{XA} + k_{AP} + k_{XP}}$$

The rate constants k_{AP} (10^4-10^5 s^{-1}) and k_{XP} (10^3 s^{-1}) are much lower than k_{AX} (~10^7 s^{-1}). According to Sétif and Brettel (1993) k_{XA} can be comparable to k_{AX} due to redox equilibrium between A_1 and F_X. Hence, the contribution of the fast component in the case of the isolated P_{700}-F_X core should not be higher than 0.1-1%, which is much lower than seen in the experiment (~10%). Therefore, an alternative explanation that assumes lack of electron transfer to F_X in a fraction of center is more likely. This may have different mechanisms in different cases.

a) *The F_X cluster is missing.* Rodday et al. (1995) have recently observed three components with half-times of 100 μs (63%), 1.2 ms (18%), and 30 ms (19%) in F_{700}-F_X cores isolated by urea treatment of *Chlamydomonas reinhardtii* TX-PS I complexes. The 100-μs component was ascribed to the back-reaction from A_1^-, and because further incubation of the sample with iron and sulfur in the presence of β-mercaptoethanol led to a decrease of the amplitude of the 100-μs component, it was suggested that some F_X was lost during the isolation procedure. In our P_{700}-F_X cores the contribution of the two fast components (20 μs and 268 μs) is <20% at saturating flash energies. However, these components are still present in P_{700}-F_X cores at under-saturating flash energies (Fig. 7), which do not induce any tens-of-milliseconds ΔA_{820} in DM-PS I complex (Fig. 5). This excludes the possibility of F_X initially missing in a subpopulation of the integral PS I complexes. On the other hand, the contribution of components decaying on tens-of-microseconds time scale found in this study is higher (~30%) than in the work of Rodday et al. (1995). This implies that treatment of the samples with urea leading to a more complete dissociation of the PsaC protein may also result in partial dissociation of the F_X cluster, which is manifest by the displacement of the 1.4-ms component with faster phases.

b) *Partial reduction of F_X cluster.* A 10-μs component appears at moderate flash intensities even in the presence of as low as 2 mM dithionite added in the dark at pH 6.3 (mild reducing conditions used for consecutive photoreduction of F_A and F_B). At more reducing conditions (dithionite at pH 10) the contribution of this component is higher, which is consistent with previous findings of Sétif and Bottin (1989), indicating partial reduction of the F_X cluster in similar conditions.

c) *Low quantum efficiency or blockage of electron transfer to F_X in a fraction of centers.* The P_{700}^+ A_1^- recombination was observed at cryogenic temperatures in higher plant PS I complexes in the presence of prereduced F_A and F_B, but oxidized F_X (Brettel et al., 1986). It was suggested recently that blockage of electron transfer to F_X in a fraction of isolated trimeric PS I complexes occurs at temperatures <200 K due to existence of PS I complexes frozen in different conformations (Schlodder et al., 1995). At room temperature, however, the electron transfer to the iron-sulfur clusters was found almost 100% efficient, as in our experiments with similar preparations (this work). It is possible, therefore, that removal of PsaC protein changes the ratio between these conformations in a way that a fraction becomes incapable of F_X photoreduction at room temperature. Another example of a decreased capacity of electron transfer through F_X cluster is represented by $C565S_{PsaB}$ and $C556S_{PsaB}$ mutants, which provide one oxygen ligand to the [4Fe-4S] cluster (Vassiliev et al., 1995a). In these mutants the contribution of components arising both from F_X^- and A_1^- is considerably increased, even at undersaturating flash energies down to 1 mJ (Vassiliev et al., 1995b), which is low enough to prevent formation of ^{3}Chl even in the P_{700}-A_1 core. Therefore, some biochemical modification of the F_X cluster microenvironment during the isolation of P_{700}-F_X core from the wild-type material can possibly also lead to an increase of the A_1^- back-reaction contribution.

The assignments made in a number of previous studies regarding the origin of the components decaying in the hundreds-of-μs time domain have been controversial. In this work, we have used one instrument setup to monitor the ΔA_{820} kinetics in isolated integral PS I complexes, with reduced F_A and F_B, P_{700}-F_X cores, and isolated P_{700}-A_1 cores. Based on results of this and a previous investigation (Brettel and Golbeck, 1995), we conclude that the A_1^- back-reaction is represented by components with lifetimes of ~10 μs and 100 μs. Therefore, the slower components found in the absence of F_A and F_B photochemistry should be assigned to F_X. Based on results from both ΔA_{820} and electric potential measurements, it seems very likely that this back-reaction is also biphasic, with lifetimes of ~300-450 μs and 1–1.5 ms. The ratio of these components' amplitudes is, however, not the same for ΔA_{820} and $\Delta\psi$ kinetics, and varies upon experimental conditions. Although the 20-μs component seen in the isolated P_{700}-F_X core is definitely related to a minority of centers not undergoing F_X photochemistry, and the major 1.4-ms component represents the F_X^- back-reaction, the interpretation of the origin of the 268-μs component is not so straightforward. On one hand, it can be interpreted as a second (faster and minor) phase of F_X^- back-reaction, but also it can represent the slower phase of A_1^- back-reaction in the above-mentioned minority of centers. It should be also noted that the major phase of the F_X^- back-reaction is slower in the isolated core than the major phase monitored with reduced F_A^- and F_B^-. This may be explained by acceleration of back-reaction in the latter case due to electrostatic repulsion from the reduced terminal iron-sulfur clusters. Indeed, a shorter lifetime has been consistently observed for the back-reaction of F_X in the presence of reduced F_A and F_B (Golbeck et al., 1988; Parrett et al., 1989; Rodday et al., 1995; this work).

At this point the most reasonable speculation we can put forward concerning biexponential back-reaction kinetics of either of studied acceptors is conformational heterogeneity existing within a population of PS I preparations. The 100-μs and 500-μs components could be discriminated only at a good signal-to-noise ratio and a relatively wide (at least 10 μs to several ms) acquisition time domain, but attempts to fit with fewer than four components with lifetimes in this range have yielded considerably poorer results, and the variations in the values of the components between preparations were higher than in the case of a four-exponential approximation in the μs-to-ms time domain.

Contribution of ^{3}Chl decay

In PS I centers with partial blockage or inefficiency of electron transfer, there exists a tens-of-μs component in addition to the inherent back-reactions from A_1^- and/or F_X^-. Two possible origins of the PS I kinetics can be considered: a) relaxation of triplet states of P_{700}, and b) relaxation of triplet states of antenna chlorophyll. A faster back-reaction from A_1^- (250- to 750-ns half-time) was shown to proceed via the $^3P_{700}$, which was followed by a slower μs-time scale decay of $^3P_{700}$ (Sétif and Bottin, 1989; Sétif and Brettel, 1990), but a later investigation provided spectroscopic evidence against participation of $^3P_{700}$ in the A_1^- back-reaction in the absence of F_A and F_B (Warren et al., 1993). On the other hand, the fast phases (with a major 10-μs component) have a significantly different flash energy dependency from the $[F_A/F_B]^-$ component(s), the magnitude of these fast phases not being saturated even at 150 mJ, the highest flash energies applied. This fact strongly argues for the second mechanism, where the appearance of the tens-of-μs decay in the presence of a saturating background illumination can be explained, as in the experiments of Nujis et al. (1986), by relaxation of the excited states of inner antenna chlorophyll molecules (formed upon a strong green excitation) via the ^{3}Chl state. According to current X-ray structure data, the PS I complex contains 64 antenna chlorophyll molecules with center-to-center distances ranging from 9 to 16 Å, whereas the center-to-center distance in the P_{700} dimer is 7 Å (Fromme et al., 1996). If the nearby antenna chlorophylls are capable of forming dimers, then the lifetimes of their triplet states should differ from those of the monomers, as in the case of Chl molecules in solution (Mathis and Sétif, 1981). Therefore, the polyphasic kinetics of ^{3}Chl decay, observed particularly upon high-energy excitation of P_{700}-A_1 core in the presence of background illumination (Fig. 11), may be related to existence of Chl molecules differing in their aggregation state. Because selective excitation of P_{700} at 710 nm likely leads to a much lower yield of antenna ^{3}Chl than excitation at 532 nm (Shuvalov et al., 1986), resolution of the μs-to-s time scale kinetics upon far-red flash excitation is necessary for a better understanding of the ΔA_{820} mechanisms in different PS I preparations.

Optimization of the instrumental setup for ΔA_{820} measurements

The results of these studies on different types of PS I preparations, including thylakoid membranes, isolated PS I complexes, and PS I cores provide a rationale for the identification of functional electron acceptors based on the kinetics of near infra-red absorbance changes of P_{700}^+. The complications include multiple kinetic components attributed to a particular acceptor, the issue of species- or kingdom-dependent equilibrium between F_X and A_1 (Sétif and Brettel, 1993), and the wide range of back-reactions available in PS I. Hence, a better assessment of electron transfer can be achieved by monitoring the kinetics on several decades of time scale, rather than making separate measurements in relatively narrow time windows. The second advantage of this approach is that in many cases the results can be evaluated even before the multiexponential fit, as placing the kinetics on the multidecade scale does not require using different scales to display traces that have their major decay components in different time domains. In terms of analysis of PS I mutants, the whole multiexponential decomposition signature, rather than individual values of parameters, should be better used for characterization of electron transport activity. Taking into account possible contribution of ^{3}Chl to the decay signal in the μs time domain, optimization of the experimental protocol for excitation energy is equally important.

The authors thank Dr. V. P. Shinkarev and Dr. A. Ya. Mulkidjanian for helpful discussions and Dr. K. N. Gourovskaya for assistance in the electric potential measurements.

This work was supported by grants from the National Science Foundation MCB#9205756 (J.H.G.) and the Russian Foundation for Fundamental Research #94-4 13094-a (A.Yu.S.).

REFERENCES

Anderson, S. L., and L. McIntosh. 1991. Partial conservation of the 5′ *ndhE-psaC-ndhD* 3′ gene arrangement of chloroplasts in the cyanobacterium *Synechocystis* sp. *PCC*. 6803: implications for NDH-D function in cyanobacteria and chloroplasts. *Plant Mol. Biol.* 16:487–499.

Baciou, L., and P. Sebban. 1995. Heterogeneity of the quinone electron acceptor system in bacterial reaction centers. *Photochem. Photobiol.* 62:271–278.

Bottin, H., P. Sétif, and P. Mathis. 1987. Study of the PS I acceptor side by double and triple flash experiments. *Biochim. Biophys. Acta.* 894: 39–48.

Brettel, K. 1989. New assignment for the 250 μs kinetics of Photosystem I: P-700$^+$ recombines with A_1^- (not F_X^-). *Biochim. Biophys. Acta.* 976: 246–249.

Brettel, K., and J. H. Golbeck. 1995. Spectral and kinetic characterization of electron acceptor A_1 in a Photosystem I core devoid of iron-sulfur centers F_X, F_B and F_A. *Photosynth. Res.* 45:183–193.

Brettel, K., P. Sétif, and P. Mathis. 1986. Flash-induced absorption changes in Photosystem I at low temperature: evidence that the electron acceptor A_1 is vitamin K_1. *FEBS Lett.* 203:220–224.

Chitnis, P. R., Q. Xu, V. P. Chitnis, and R. Nechushtai. 1995. Function and organization of Photosystem I polypeptides. *Photosynth. Res.* 44:23–40.

Drachev, L. A., A. D. Kaulen, A. Y. Semenov, I. I. Severina, and V. P. Skulachev. 1979. Lipid-impregnated filters as a tool for studying the electric current-generating proteins. *Anal. Biochem.* 96:250–262.

Fromme, P., H. T. Witt, W. D. Schubert, O. Klukas, W. Saenger, and N. Krauß. 1996. Structure of Photosystem I at 4.5 Å resolution: a short review including evolutionary aspects. *Biochim. Biophys. Acta.* 1275: 76–83.

Gao, J.-L., R. J. Shopes, and C. A. Wraight. 1991. Heterogeneity of kinetics and electron transfer equilibria in the bacteriopheophytin and quinone acceptors of reaction centers from *Rhodopseudomonas viridis*. *Biochim. Biophys. Acta.* 1056:259–272.

Gerken, S., J. P. Dekker, E. Schlodder, and H. T. Witt. 1989. Studies on the multiphasic charge recombination between chlorophyll a_{II}^+ (P-680$^+$) and plastoquinone Q_A^- in Photosystem II complexes. Ultraviolet difference spectrum of Chl-a_{II}+/Chl-a_{II}. *Biochim. Biophys. Acta.* 977:52–61.

Golbeck, J. H. 1995. Resolution and reconstitution of Photosystem I. *In* CRC Handbook of Organic Photochemistry and Photobiology. CRC Press, Boca Raton, Florida. 1407–1419.

Golbeck, J. H., and J. M. Cornelius. 1986. Photosystem I charge separation in the absence of centers A and B. I. Optical characterization of center 'A_2' and evidence for its association with a 64-kDa peptide. *Biochim. Biophys. Acta.* 849:16–24.

Golbeck, J. H., K. G. Parrett, T. Mehari, K. L. Jones, and J. J. Brand. 1988. Isolation of the intact Photosystem I reaction center core containing P700 and iron-sulfur center F_X. *FEBS Lett.* 228:268–272.

Hastings, G., S. Hoshina, A. N. Webber, and R. E. Blankenship. 1995. Universality of energy and electron transfer processes in Photosystem I. *Biochemistry.* 34:15512–15522.

Hiyama, T., and B. Ke. 1972. Difference spectra and extinction coefficients of P700. *Biochim. Biophys. Acta.* 267:160–171.

Jung, Y.-S., L. Yu, and J. H. Golbeck. 1995. Reconstitution of iron-sulfur center F_B results in complete restoration of NADP$^+$ photoreduction in Hg-treated Photosystem I complexes from *Synechococcus* sp. *PCC 6301. Photosynth. Res.* 46:249–255.

Ke, B. 1972. One-way electron discharge subsequent to the photochemical charge separation in Photosystem I. *Biochim. Biophys. Acta.* 267: 595–599.

Kojima, Y., Y. Niinomi, S. Tsuboi, T. Hiyama, and H. Sakurai. 1987. Destruction of Photosystem I iron-sulfur centers of spinach and *Anacystis nidulans* by mercurials. *Bot. Mag.* 100:243–253.

Leibl, W., B. Toupance, and J. Breton. 1995. Photoelectric characterization of forward electron transfer to iron-sulfur centers in Photosystem I. *Biochemistry.* 34:10237–10244.

Li, N., P. V. Warren, J. H. Golbeck, G. Frank, H. Zuber, and D. A. Bryant. 1991. Polypeptide composition of the Photosystem I complex and the Photosystem I core protein from *Synechococcus* sp. *PCC 6301. Biochim. Biophys. Acta.* 1059:215–225.

Lüneberg, J., P. Fromme, P. Jekow, and E. Schlodder. 1994. Spectroscopic characterization of PS I core complexes from thermophilic *Synechococcus* sp.—identical reoxidation kinetics of A_1^- before and after removal of the iron-sulfur-clusters F_A and F_B. *FEBS Lett.* 338:197–202.

Mamedov, M. D., R. M. Gadzhieva, L. A. Drachev, A. A. Zaspa, and A. Y. Semenov. 1995. Generation of electric potential in proteoliposomes containing PS1 complexes from cyanobacteria. *Biochemistry-Moscow (Engl. Tr.).* 60:565–568.

Mathis, P., and P. Sétif. 1981. Near infra-red absorption spectra of the chlorophyll *a* cations and triplet state in vitro and in vivo. *Isr. J. Chem.* 21:316–320.

Nuijs, A. M., V. A. Shuvalov, H. J. Van Gorkom, J. J. Plijter, and L. N. M. Duysens. 1986. Picosecond absorbance difference spectroscopy on the primary reactions and the antenna-excited states in Photosystem I particles. *Biochim. Biophys. Acta.* 850:310–318.

Parrett, K. G., T. Mehari, and J. H. Golbeck. 1990. Resolution and reconstitution of the cyanobacterial Photosystem I complex. *Biochim. Biophys. Acta.* 1015:341–352.

Parrett, K. G., T. Mehari, P. G. Warren, and J. H. Golbeck. 1989. Purification and properties of the intact P-700 and F_X-containing Photosystem I core protein. *Biochim. Biophys. Acta.* 973:324–332.

Rodday, S. M., A. N. Webber, S. E. Bingham, and J. Biggins. 1995. Evidence that the F_X domain in Photosystem I interacts with the subunit PsaC-Site-directed changes in PsaB destabilize the subunit interaction in *Chlamydomonas reinhardtii. Biochemistry.* 34:6328–6334.

Rubin, A. B., and V. P. Shinkarev, 1984. Electron transfer in biological systems, Chapter 12 (in Russian). Nauka, Moscow.

Sakurai, H., K. Inoue, T. Fujii, and P. Mathis. 1991. Effects of selective destruction of iron-sulfur center B on electron transfer and charge recombination in Photosystem I. *Photosynth. Res.* 27:65–71.

Sauer, K., S. Acker, P. Mathis, and J. A. Van Best. 1977. Optical studies of photosystem I particles: evidence for the presence of multiple electron acceptors. *Dev. Bioenerg. Biomembr.* 1:351–359.

Sauer, K., P. Mathis, S. Acker, and J. A. Van Best. 1978. Electron acceptors associated with P-700 in Triton solubilized photosystem I particles from spinach chloroplasts. *Biochim. Biophys. Acta.* 503: 120–134.

Sauer, K., P. Mathis, S. Acker, and J. A. Van Best. 1979. Absorption changes of P-700 reversible in milliseconds at low temperature in Triton-solubilized photosystem I particles. *Biochim. Biophys. Acta.* 545: 466–472.

Schlodder, E., K. Brettel, K. Falkenberg, and M. Gergeleit. 1995. Temperature dependence of the reoxidation kinetics of A_1^- in PS I. *In* Photosynthesis: From Light to Biosphere, Vol. 2. P. Mathis, editor. Kluwer Acad. Publ., Dordrecht. 107–110.

Sétif, P. 1992. Energy transfer and trapping in Photosystem I. *In* The Photosystems: Structure, Function and Molecular Biology. Elsevier Science Publishers B.V., Amsterdam. 471–499.

Sétif, P., and H. Bottin. 1989. Identification of electron-transfer reactions involving the acceptor A_1 of Photosystem I at room temperature. *Biochemistry.* 28:2689–2697.

Sétif, P., and K. Brettel. 1990. Photosystem I photochemistry under highly reducing conditions: study of the P700 triplet state formation from the secondary radical pair (P700$^+$-A_1^-). *Biochim. Biophys. Acta.* 1020: 232–238.

Sétif, P., and K. Brettel. 1993. Forward electron transfer from phylloquinone-A_1 to iron sulfur centers in spinach Photosystem-I. *Biochemistry.* 32:7846–7854.

Sétif, P., G. Hervo, and P. Mathis. 1981. Flash-induced absorption changes in photosystem I. Radical pair or triplet state formation? *Biochim. Biophys. Acta.* 638:257–267.

Shinkarev, V. P., and C. A. Wraight. 1993. Electron and proton transfer in the acceptor quinone complex of reaction centers of phototrophic bacteria. *In* The Photosynthetic Reaction Center, Vol. 1. J. Deisenhofer and J. Norris, editors. Academic Press, New York. 193–255.

Shuvalov, V. A., A. M. Nuijs, H. J. Van Gorkom, H. W. J. Smit, and L. N. M. Duysens. 1986. Picosecond absorbance changes upon selective excitation of the primary electron donor P-700 in Photosystem I. *Biochim. Biophys. Acta.* 850:319–323.

Sigfridsson, K., Ö. Hansson, and P. Brzezinski. 1995. Electrogenic light reactions in Photosystem 1. Resolution of electron-transfer rates between the iron-sulfur centers. *Proc. Natl. Acad. Sci. USA.* 92:3458–3462.

Smart, L., S. Anderson, and L. McIntosh. 1991. Targeted genetic inactivation of the Photosystem-I reaction center in the cyanobacterium *Synechocystis* sp. *PCC-6803. EMBO J.* 10:3289–3296.

Vassiliev, I. R., Y.-S. Jung, L. B. Smart, R. Schulz, L. McIntosh, and J. H. Golbeck. 1995a. A mixed ligand iron-sulfur cluster (C556S$_{PsaB}$ or C565S$_{PsaB}$) in the F_X-binding site leads to a decreased quantum efficiency of electron transfer in photosystem I. *Biophys. J.* 69:1544–1553.

Vassiliev, I. R., Y.-S. Jung, R. Schulz, L. B. Smart, L. McIntosh, and J. H. Golbeck. 1995b. Electron Transfer via the F_X cluster of PS I in PsaB mutants of *Synechosystis* sp. *PCC.* 6803. *In* Photosynthesis: From Light to Biosphere, Vol. 2. P. Mathis, editor. Kluwer Acad. Publ., Dordrecht. 131–134.

Warren, P. V., J. H. Golbeck, and J. T. Warden. 1993. Charge recombination between P700$^+$ and A_1^- occurs directly to the ground state of P700 in a Photosystem I core devoid of F_X, F_B, and F_A. *Biochemistry.* 32:849–857.

Warren, P. V., K. G. Parrett, J. T. Warden, and J. H. Golbeck. 1990. Characterization of a photosystem I core containing P700 and intermediate electron acceptor A_1. *Biochemistry.* 29:6545–6550.

Yu, J., I. R. Vassiliev, Y.-S. Jung, J. H. Golbeck, and L. McIntosh. 1996. Strains of *Synechocystis* sp. *PCC.* 6803 with altered PsaC. I. Mutations incorporated in the cysteine ligands of the two [4Fe-4S] clusters F_A and F_B of Photosystem I. *J. Biol. Chem.* (in press).